

## Two Dimensional Si-Based Semiconductor Si<sub>1-y</sub>C<sub>y</sub> : C Atom Induced Band Structure Modulation at Visible Region

T. Mizuno, Y. Nagamine, U. Omata, Y. Suzuki, W. Urayama, T. Aoki, and T. Sameshima\*

Kanagawa Univ., Hiratsuka, Japan ([mizuno@info.kanagawa-u.ac.jp](mailto:mizuno@info.kanagawa-u.ac.jp)), \*Tokyo Univ. of Agric. and Tech., Koganei, Japan

### Abstract

We experimentally studied C atom impact on band structure modulation in 2D silicon carbon alloy Si<sub>1-y</sub>C<sub>y</sub> fabricated by hot C<sup>+</sup> ion implantation into (100) SOI substrate in a wide range of  $Y$ . Photoluminescence (PL) method shows that bandgap  $E_G$  and PL intensity  $I_{PL}$  of 2D-Si<sub>1-y</sub>C<sub>y</sub> drastically increase with increasing  $Y$  in high  $Y$  ( $\geq 0.003$ ), and thus we demonstrated higher  $E_G$  of 2.5eV and the visible  $I_{PL}$  of wavelength  $\lambda$  less than 500nm. In addition, graphitic C peak at 1500cm<sup>-1</sup> is also confirmed at  $Y=0.07$  by UV-Raman analysis. However, even in low  $Y$  ( $<10^{-3}$ ),  $I_{PL}$  of 2D-Si<sub>1-y</sub>C<sub>y</sub> also increase with increasing  $Y$ , which is caused by the compressive strain, but  $Y$  dependence of  $E_G$  is very small. Thus,  $E_G$  of 2D-Si<sub>1-y</sub>C<sub>y</sub> can be controlled by 2D-Si<sub>1-y</sub>C<sub>y</sub> thickness  $d_S$  and  $Y$ .

### 1. Introduction

2D Si layer is a key technology for realizing extremely-thin SOIs (ETSOIs) and FinFET CMOS [1], as well as Si photonics [2]. We experimentally demonstrated phonon confinement effects (PCE) and  $E_G$  expanding due to electron confinement [3]-[5] in 2D-Si layers. A PL peak photon energy  $E_{PH}$  of a fully relaxed (100)2D-Si layer without a surface oxide [5] agrees well with theoretical  $E_G$  value [6]. Thus,  $E_G$  of (100)2D-Si can be precisely obtained by PL method.

$E_G$  of (100)2D-Si can be controlled by  $d_S$  [5], [6], but is still lower than 1.9eV whose  $\lambda$  is longer than 650nm. However, to realize visible Si photonics as well as source hetero structures (SHOT) which can inject high velocity carrier into channel from high  $E_G$  source regions [7], [8], it is necessary to develop a new technology for higher  $E_G$  without controlling  $d_S$ . In 3D-Si<sub>1-y</sub>C<sub>y</sub>,  $E_G$  can increase with increasing  $Y$  [9]-[11], and PL intensity  $I_{PL}$  also increases with increasing  $Y$  [9]. Therefore, 2D-Si<sub>1-y</sub>C<sub>y</sub> is a new candidate for  $E_G$  and  $\lambda$  engineering for future CMOS and Si-photonics.

In this work, we experimentally studied the impact of  $Y$  on  $E_G$  modulation of 2D-Si<sub>1-y</sub>C<sub>y</sub> fabricated by <sup>12</sup>C<sup>+</sup> hot ion-implantation into (100)SOIs. We obtained the  $Y$  dependence of  $E_G$  modulation of 2D-Si<sub>1-y</sub>C<sub>y</sub> by PL method in a wide range of  $Y$  ( $10^{-5} < Y \leq 0.07$ ), and demonstrated higher  $E_G$  of 2.5eV and visible  $\lambda$ .

### II. Experiment for 2D-Si<sub>1-y</sub>C<sub>y</sub> by Hot C<sup>+</sup> Implantation

High quality 2D-Si<sub>1-y</sub>C<sub>y</sub> layers with a wide range of  $Y$  were fabricated by the combination of 1) <sup>12</sup>C<sup>+</sup> hot ion implantation technique [12] into (100) bonded SOI substrate at higher than 900°C, and 2) two-step (low-temperature  $T$  after high- $T$  oxidation) thermal oxidation technique [3] (Fig.1). 0.5-nm thick 2D-Si<sub>1-y</sub>C<sub>y</sub> layers with  $10^{-5} < Y \leq 0.07$  were successfully formed in this work.

SIMS analysis (Fig.2) shows that carbon density  $N_C$  in 8.5nm Si locally condenses at two interfaces of the BOX and SiO<sub>2</sub>. However, in a  $d_S$  (=distance between the two interfaces) limited case of 2D-Si,  $N_C$  of 2D-Si can be assumed to be peak  $N_C$  value at the interface and uniform. Peak  $N_C$  rapidly decreases by oxidizing SOI, because of small segregation coefficients  $m_C$  of carbon at the Si/SiO<sub>2</sub> interface. The maximum and minimum  $Y$  of 0.5-nm 2D-Si<sub>1-y</sub>C<sub>y</sub> can be estimated by SIMS analysis and Eq.(1) (Fig.3 caption), and be achieved to be about 0.07 and  $10^{-5}$ , respectively, using various <sup>12</sup>C<sup>+</sup> dose ( $5 \times 10^{12} \leq D_C \leq 2 \times 10^{16}$  cm<sup>-2</sup>).

We analyzed the  $E_G$  properties of 0.5nm thick 2D-Si<sub>1-y</sub>C<sub>y</sub> layers evaluated by PL method, where excitation laser energy  $h\nu$  was varied from 2.3 to 3.8eV at room temperature [3]. Laser power  $P_L$  was set to be 1mW to compress the  $P_L$  heating of Si [3], and the laser diameter was 1μm. Phonon properties of 2D-Si<sub>1-y</sub>C<sub>y</sub> layers were measured by UV (325-nm)/visual (532-nm) Raman spectroscopy. We observe no degradation of the FWHM of Si peak even at  $D_C = 2 \times 10^{16}$  cm<sup>-2</sup>, which is the benefit of hot C<sup>+</sup> implantation technique.

### III. Large $E_G$ Modulation by C Atom

#### A. PL Si-C Peak in 2D-Si<sub>1-y</sub>C<sub>y</sub>

UV-Raman analysis shows double peaks of D and G bands of graphitic C at about 1500cm<sup>-1</sup> [11] (Fig.3) only in  $Y=0.07$ , and thus silicon-carbon alloys were successfully fabricated.

Very large and double-peak PL spectra excited by 2.3eV laser can be newly observed at  $Y \geq 0.003$  (Fig.4). The lower  $E_{PH}$  peak is

attributable to 2D-Si [3], but new higher  $E_{PH}$  is considered to be PL from the 2D Si-C alloy.  $I_{PL}$  of both Si and Si-C peaks drastically increases with increasing  $Y$  (Figs.4, 5) in  $Y \geq 0.003$ , compared to  $I_{PL}$  at  $Y=0$ ;  $I_{PL0}$ , resulting in  $I_{PL}/I_{PL0} \propto Y^{1.4}$  (2) (Fig.5). Especially,  $I_{PL}/I_{PL0}$  at  $Y=0.07$  reaches over 20, which is very suitable for Si photonics. Here,  $I_{PL} \propto \alpha\eta = \alpha/(1 + \tau_R/\tau_{NR})$  (3), where  $\alpha$ ,  $\eta$ ,  $\tau_R$ , and  $\tau_{NR}$  are absorption coefficient, luminescence efficiency, radiative, and non-radiative life times of electrons, respectively [15]. Thus, when  $\eta = \text{const.}$ ,  $\alpha$  of 2D-Si<sub>1-y</sub>C<sub>y</sub>;  $\alpha_{SC}$  is estimated to be about 26 times as large as that of 2D-Si ( $\alpha_{2D}$ ) which is also two orders of magnitude larger than that of 3D-Si ( $\alpha_{3D}$ ) [14], resulting in  $\alpha_{SC}/\alpha_{3D} \approx 3300$  (Fig.5). However, the  $I_{PL}$  at  $Y \approx 3 \times 10^{-3}$  has the minimum value (Fig.5), which is possibly due to the  $\tau_{NR}$  decrease with increasing  $Y$ , because of C<sup>+</sup> ion damage.

Moreover, PL spectrum of 2D-Si<sub>0.93</sub>C<sub>0.07</sub> in visible region strongly depends on  $h\nu$  (Fig.6), because electrons cannot be generated by lower  $h\nu$  ( $E_G > h\nu$ ). When  $h\nu = 3.8\text{eV}$ , we can newly observe visible PL spectrum. The peak  $E_{PH}$  reaches 2.5eV, resulting in peak- $\lambda \approx 500\text{nm}$ . PL spectrum tail can be also detected even in higher than 3eV. However, since the PL peak was very broad in  $Y < 0.07$ ,  $E_G$  of 2D-Si<sub>1-y</sub>C<sub>y</sub> is almost independent of  $Y$ , but is higher than  $E_G$  of 3D-Si<sub>1-y</sub>C<sub>y</sub> [9] (Fig.7). Consequently, 2D-Si<sub>1-y</sub>C<sub>y</sub> with high  $Y$  is a very promising for visible Si-photonics and SHOT.

#### B. PL Si-C Peak in 2D-Si<sub>1-y</sub>C<sub>y</sub>

Even when  $Y = 4 \times 10^{-4}$ , we can observe  $I_{PL}$  enhancement ( $I_{PL}/I_{PL0} = 1.66$ ) and  $E_G$  expanding ( $\approx 1.8\text{eV}$ ) (Fig.8). However, no PL Si-C peak was observed in  $Y < 0.001$  (Fig.8). Lattice constant 2D-Si<sub>1-y</sub>C<sub>y</sub>  $a_{SC}$  also decreases with increasing  $Y$ , compared with that of 2D-Si  $a_S$  [11]. Thus, the compressive strain  $\varepsilon_C$  in 2D-Si<sub>1-y</sub>C<sub>y</sub> increases with increasing  $Y$  (Fig.9), according to  $\varepsilon_C$  formula of 3D-Si<sub>1-y</sub>C<sub>y</sub> [11];  $\varepsilon_C(Y) = (a_S - a_{SC}(Y))/a_S = (-0.24Y + 0.057Y^2)/a_S$  (4). So, residual tensile strain  $\varepsilon_T(Y)$  of 2D-Si, which is applied by the large difference of expansion coefficient between SiO<sub>2</sub> and 2D-Si [5], can be relaxed by the equations of Eq.(4) and  $\varepsilon_T(Y) = \varepsilon_{T0} - \varepsilon_C(Y)$  (5) ( $\varepsilon_{T0}$  is the residual tensile strain (0.33%) in 0.5-nm 2D-Si) (Fig.9) without etching SiO<sub>2</sub>. Thus, using  $E_G(Y) \propto \exp((\varepsilon_{T0} - \varepsilon_C(Y))/\varepsilon_0)$  (6), where  $\varepsilon_0$  the fitting parameter (0.22%) [5],  $E_G$  rapidly increases with increasing  $Y$  even in  $Y < 10^{-3}$  (Fig.10), which can be well explained by the  $\varepsilon_T$  relaxation induced  $E_G$  expansion by Eq.(6). Thus, even small  $Y$  ( $< 10^{-3}$ ) can affect the band structure of 2D-Si<sub>1-y</sub>C<sub>y</sub>.

#### C. Device Design for High $E_G$ and Visible Photon Emission

According to the above discussions and our previous works [4], [5], it is possible to control higher  $E_G$  and shorter photon emission of 2D Si-based semiconductor, by designing only three key parameters of  $d_S$ , SiO<sub>2</sub> thickness  $T_{OX}$ , and  $Y$ . For example, when  $d_S \leq 0.5\text{nm}$  (Fig.11), thinner  $d_S$  in 2D-Si is required to realize band structures with  $1.1 < E_G \leq 2.1\text{eV}$  or  $\lambda \geq 600\text{nm}$  [4]. Especially in the case of  $1.7 < E_G \leq 2.1\text{eV}$ , the 2D-Si must be relaxed by thinning  $T_{OX}$  [5]. In addition, to realize  $E_G > 2.1\text{eV}$  ( $\lambda < 600\text{nm}$ ), a 2D silicon-carbon alloy technology is strongly necessary.

### IV. Conclusion

We experimentally studied C content effects on band structure modulation in a 0.5-nm 2D-Si<sub>1-y</sub>C<sub>y</sub> layer fabricated by C<sup>+</sup> hot ion implantation technique into (100)SOI. PL can be detected in a wide range of  $10^{-5} < Y \leq 0.07$ .  $I_{PL}$  and  $E_G$  of 2D-Si<sub>1-y</sub>C<sub>y</sub> rapidly increases with increasing  $Y$ , and  $E_G$  of 2.5eV and visible  $\lambda$  of 500-nm can be achieved at  $Y=0.07$ . Consequently, we can precisely design a future 2D device with various high- $E_G$  and visible  $\lambda$ , by controlling only three parameters of  $d_S$ ,  $T_{OX}$ , and  $Y$ .

**Acknowledgement:** We would like to thank Prof. J. Nakata and Dr. Y. Hoshino of Kanagawa Univ. for supporting carbon ion implantation.

**References:** [1] J.-P. Colinge, *SOI Tech.*, (Kluwer) 2004. [2] S. Saito, IEDM 2008, Paper 19.5. [3] T. Mizuno, JJAP 51, 02BC03, 2012. [4] T. Mizuno, JJAP 52, 04CC13, 2013. [5] T. Mizuno, JJAP 54, 4DC02, 2015. [6] B. K. Agrawal, APL 77, 3039, 2000. [7] T. Mizuno, TED 52, 2690, 2005. [8] K.-J. Chui, TED 54, 249, 2007. [9] L.R. Tessler, Phys. Rev. B, 52, 10962, 1995. [10] W. Liu, APL 78, 37, 2001. [11] S.T. Pantelides ed., *Silicon-Germanium Carbon Alloys*, (Taylor&Francis), 2002. [12] T. Mizuno, JJAP 50, 04DC02, 2011. [13] R.-P. Wang, Phys. Rev. B 61, 16827, 2000. [14] T. Mizuno, SSDM, p.96, 2013. [15] S. M. Sze, *Phys. of Semiconductor Devices* (Wiley), 2007.

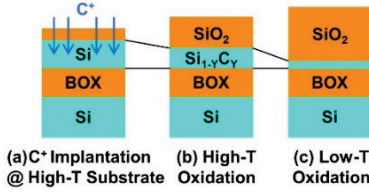


**Fig.1** Schematic fabrication for 2D-Si<sub>1-y</sub>C<sub>y</sub> layers. (a) After <sup>12</sup>C<sup>+</sup> implantation into 1000°C (100)SOI substrate, (b) Si was thinned by 1000°C oxidation.  $D_C$  was varied from  $5 \times 10^{12}$  to  $2 \times 10^{16} \text{ cm}^{-2}$ . (c) Additional 900°C oxidation was carried out to form 0.5nm-region thick Si<sub>1-y</sub>C<sub>y</sub> layer, resulting in  $10^{-5} \leq Y \leq 0.07$ .

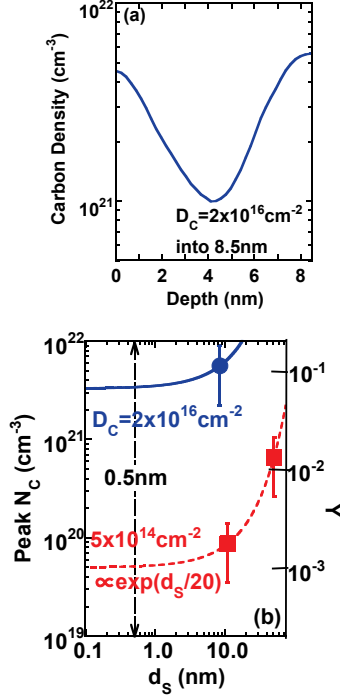


**Fig.2** (a) SIMS (solid line) results of  $N_C$  (dashed line) just after hot C<sup>+</sup> ion implantation into 8.5-nm SOI which is the minimum thickness for SIMS, where  $D_C = 2 \times 10^{16} \text{ cm}^{-2}$ . (b) Experimental peak  $N_C$  at the Si/BOX interface with error bars (about 60%) due to SIMS accuracy which is very low at the interface, where  $D_C=2 \times 10^{16}$  (circle) and  $5 \times 10^{14} \text{ cm}^{-2}$  (triangles).  $N_C$  decreases with oxidizing Si, because of the small  $m_C$  at SiO<sub>2</sub>/Si.  $d_s$  dependence of  $N_C(d_s)$  can be obtained by the following 1D-differential equation:  $dN_C/dx \propto N_C(x)$  resulting in  $N_C(d_s) = N_0 \exp(ds/d_0)$  (1) (solid line), where  $N_0$  which depends on  $D_C$  and fitting  $d_0$  (=20nm) is constant. Solid and dashed lines show the estimated  $d_s$  dependence of peak  $N_C$  by Eq.(1). As a result, the right axis shows that the maximum  $Y$  was 0.07 at  $d_s=0.5\text{nm}$ .

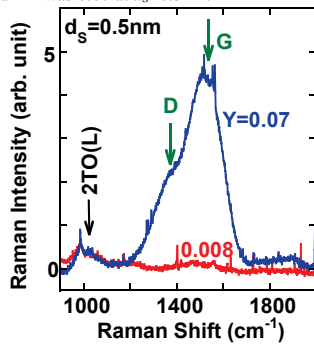


**Fig.3** UV-Raman spectra at  $Y$  of 0.07 (blue line) and 0.008 (red line), where  $d_s=0.5\text{nm}$ . Double Raman peaks at  $Y=0.07$  are attributable to D (1340 $\text{cm}^{-1}$ ) and G (1500 $\text{cm}^{-1}$ ) bands of graphitic C [11], whereas low  $Y$  sample shows no C band. Raman peak at about 1000 $\text{cm}^{-1}$  shows the phonon mode of Si 2TO(L) [13].

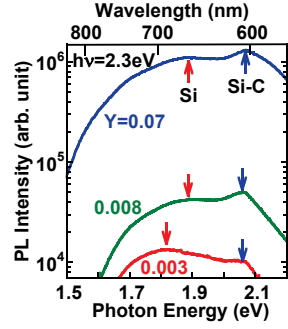


**Fig.4** PL spectra excited by 2.3eV laser as a function of  $Y$  at  $Y \geq 0.003$  condition, where  $d_s=0.5\text{nm}$ . Lower and upper axes show PL photon energy and wavelength, respectively. Arrows show peak  $I_{PL}$  which are attributable to Si and Si-C alloy.

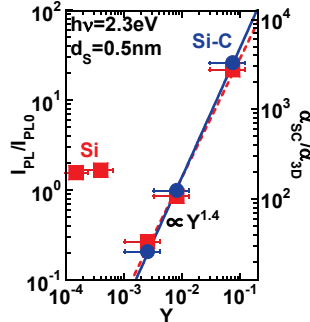


**Fig.5** Peak  $I_{PL}$  of 2D-Si<sub>1-y</sub>C<sub>y</sub> normalized by that of 2D-Si;  $I_{PL0}$  vs.  $Y$ , where  $h\nu=2.3\text{eV}$  and  $d_s=0.5\text{nm}$ . The right axis shows the estimated  $\alpha_{SC}$  of 2D-Si<sub>1-y</sub>C<sub>y</sub> normalized by  $\alpha_{SD}$  of 3D-Si. Circles and squares show Si-C and Si peaks, respectively. Solid and dashed lines show the fitting curves of  $I_{PL} \propto Y^{1.4}$  in  $Y > 10^{-3}$ , where the correlation coefficient was about 1. Error bars show the  $Y$  accuracy (60%) obtained by SIMS.

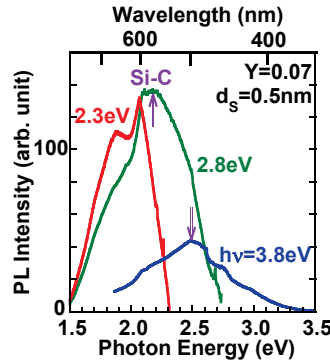


**Fig.6** Excitation laser energy dependence of PL spectra at  $Y=0.07$  in visible region, where  $d_s=0.5\text{nm}$ . Blue, green, and red lines show the data excited by  $h\nu$  of 3.8, 2.8, and 2.3eV, respectively.

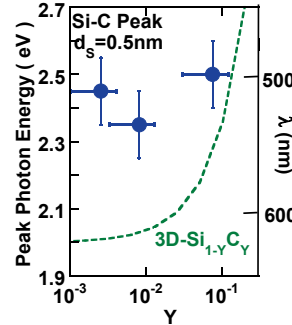


**Fig.7**  $Y$  dependence of  $E_G$  (left axis) and  $\lambda$  (right axis) at Si-C peak (circles), where  $h\nu=3.8\text{eV}$  and  $d_s=0.5\text{nm}$ . Dashed line shows the data of 3D-Si<sub>1-y</sub>C<sub>y</sub> [9].

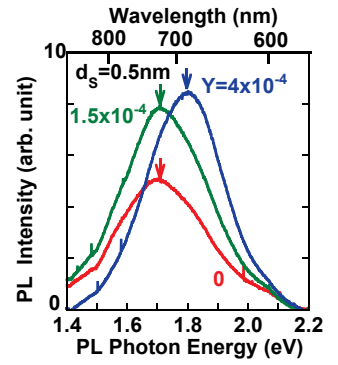


**Fig.8** PL spectra as a function of  $Y$  in low  $Y$  condition ( $\leq 4 \times 10^{-4}$ ), where  $h\nu=2.3\text{eV}$  and  $d_s=0.5\text{nm}$ .  $I_{PL}$  also increases with increasing  $Y$ , and  $E_G$  at  $Y=4 \times 10^{-4}$  increases even at  $Y < 0.1\%$ .

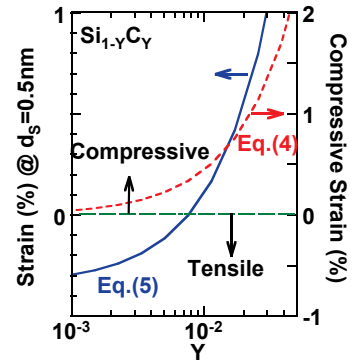


**Fig.9**  $Y$  dependence of estimated strain (solid line) of 0.5nm Si<sub>1-y</sub>C<sub>y</sub> by Eq.(5) and calculated compressive-strain (dashed line) of 3D-Si<sub>1-y</sub>C<sub>y</sub> [11] by Eq.(4).

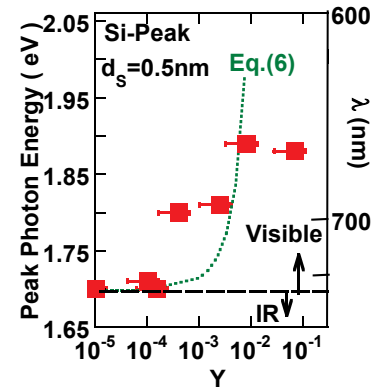


**Fig.10**  $Y$  dependence of  $E_G$  (left axis) and  $\lambda$  (right axis) at peak  $I_{PL}$  of Si (squares), where  $h\nu=2.3\text{eV}$  and  $d_s=0.5\text{nm}$ . Dotted lines show the tensile strain dependence of  $E_G$  model in 2D-Si<sub>1-y</sub>C<sub>y</sub> by Eq.(6).

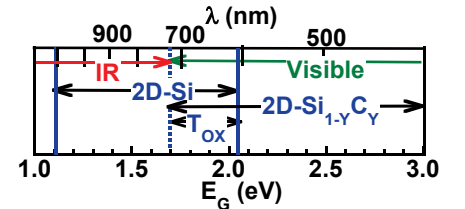


**Fig.11** Device design for realizing higher  $E_G$  and visible  $\lambda$  in 2D-Si<sub>1-y</sub>C<sub>y</sub> and 2D-Si, where  $d_s \geq 0.5\text{nm}$ . Lower and upper axes show  $E_G$  and  $\lambda$ , respectively. There are only three key parameters of  $d_s$ ,  $T_{ox}$ , and  $Y$  for realizing various  $E_G$  in 2D-Si device.